Check for updates

JGR Planets

RESEARCH ARTICLE
10.1029/2023JE007777

The Proximal Ejecta Around the Marine-Target Lockne Impact Structure, Sweden

Erik Sturkell[1], Jens Ormö[2], Eric Austin Hegardt[1], Gabrielle Stockmann[3], Erik Meland[4], and Torbjörn Wikström[5]

[1]Department of Earth Sciences, University of Gothenburg, Goteborg, Sweden, [2]Centro de Astrobiología (CAB), INTA-CSIC, Instituto Nacional de Técnica Aeroespacial, Torrejón de Ardoz, Spain, [3]Jarvik Geoconsulting AB, Gothenburg, Sweden, [4]Olofstorp, Sweden, [5]Stjärnsund, Sweden

Key Points:

- The Lockne marine impact structure uniquely preserves its proximal ejecta blanket
- The well-preserved proximal ejecta represents roughly 26 vol% of the calculated excavated volume of crystalline rocks
- The structure and its ejecta reveal the sequence of events that take place when an asteroid hits a marine, sediment, and crystalline target

Supporting Information:

Supporting Information may be found in the online version of this article.

Correspondence to:

E. Sturkell,
erik.sturkell@gvc.gu.se

Citation:

Sturkell, E., Ormö, J., Hegardt, E. A., Stockmann, G., Meland, E., & Wikström, T. (2023). The proximal ejecta around the marine-target Lockne impact structure, Sweden. *Journal of Geophysical Research: Planets*, *128*, e2023JE007777. https://doi.org/10.1029/2023JE007777

Received 19 FEB 2023
Accepted 6 JUL 2023

© 2023. The Authors.
This is an open access article under the terms of the Creative Commons Attribution-NonCommercial-NoDerivs License, which permits use and distribution in any medium, provided the original work is properly cited, the use is non-commercial and no modifications or adaptations are made.

Abstract Very few impact craters on Earth have preserved proximal ejecta (ejecta blanket), which when present help us to better understand the cratering processes when asteroid hits Earth. The 458 Ma old Lockne impact structure consists of a 7.5-km wide nested crater in the crystalline basement surrounded by an approximately 3-km wide brim developed in the upper sedimentary target. The asteroid struck a marine environment with 500 m sea water, 50-m lithified limestone, and 30 m of Cambrian clay covering a peneplainized crystalline basement. The transient crater that developed in rock and water obtained a "soup-plate" shape and reached about 7 km from the impact crater center, the farthest on the down-range side. The brim of the soup-plate was partially stripped of Ordovician limestone and water before the emplacement of inner impact crater ejecta. Most of the ejecta rest upon the Cambrian clay (today shale). The asteroid struck obliquely from the east, which is reflected in the ejecta distribution. The proximal ejecta field is divided into two crescent-shaped areas to the northwest and southwest of the nested crater and covers 26 km^2. Resistivity profiles, mapping, and core drilling show that the thickness of the ejecta masses range between 30 and 50 m with a total volume of about 1 km^3. They were not re-worked by the resurge. They represent roughly 26 vol% of the calculated excavated volume of crystalline rocks. Thus, it can be concluded that the Lockne impact crater has a well-preserved ejecta blanket.

Plain Language Summary Very few terrestrial impact structures have preserved ejecta blankets. Generally, the strong erosion affecting Earth's surface, and the often frail character of the ejected material, hampers their preservation. Despite its high age of 458 million years, the Lockne impact structure is a rare exception due to a combination of a target with 500 m of seawater, 80 m of limestone, and 30 m of clay resting on a flat granitic basement, and rapid burial by subsequent marine sedimentation. The seawater was expelled outward, and the expanding crater reached deep into the basement. Limestone surrounding the basement crater was blasted off like a carpet. The impact structure obtained a "soup-plate" shape with a 7.5 km wide nested crater in the basement surrounded by a 3.5-km wide, shallow "brim." The more difficultly mobilized clay and exposed basement rock of the brim got bombarded by granitic ejecta forming a blanket. After less than 2 min, the 2 km high water wall collapsed and water rushed back to flood the dry impact crater, leaving only larger ejecta fragments and more consolidated parts of the ejecta blanket. This sequence of events only occurs in marine and stratified target settings, such as at Lockne.

1. Introduction

Except for some impact structures on low-gravity cosmic bodies, essentially all fresh impact structures are surrounded by ejecta from the crater interior (Melosh, 1989, p. 89). The geological activity on Earth does not favor the preservation of ejecta deposits. The preservation varies considerably. The best-preserved exposed ejecta deposits according to Osinski et al. (2011) are the Mauritanian Tenoumer structure (1.9 km diameter, 0.0214 Ma) and Pingualuit (New Quebec) in Canada (3.4 km diameter, 1.4 Ma). In Table 1 in Osinski et al. (2011), nine additional structures with preserved ejecta deposits are listed. Several other structures are completely buried and can only be observed with drilling and for these, the precise extent of the ejecta deposits is difficult to estimate. Also, there are ejecta deposits without a known impact structure. In this aspect, the Lockne structure offers a unique opportunity to study and explore the proximal ejecta (the ejecta blanket) around a marine target impact. The preservation of the crater and its proximal ejecta is favored by a combination of a relatively young age and large magnitude of the event (making a large impact crater), as well as that it occurred

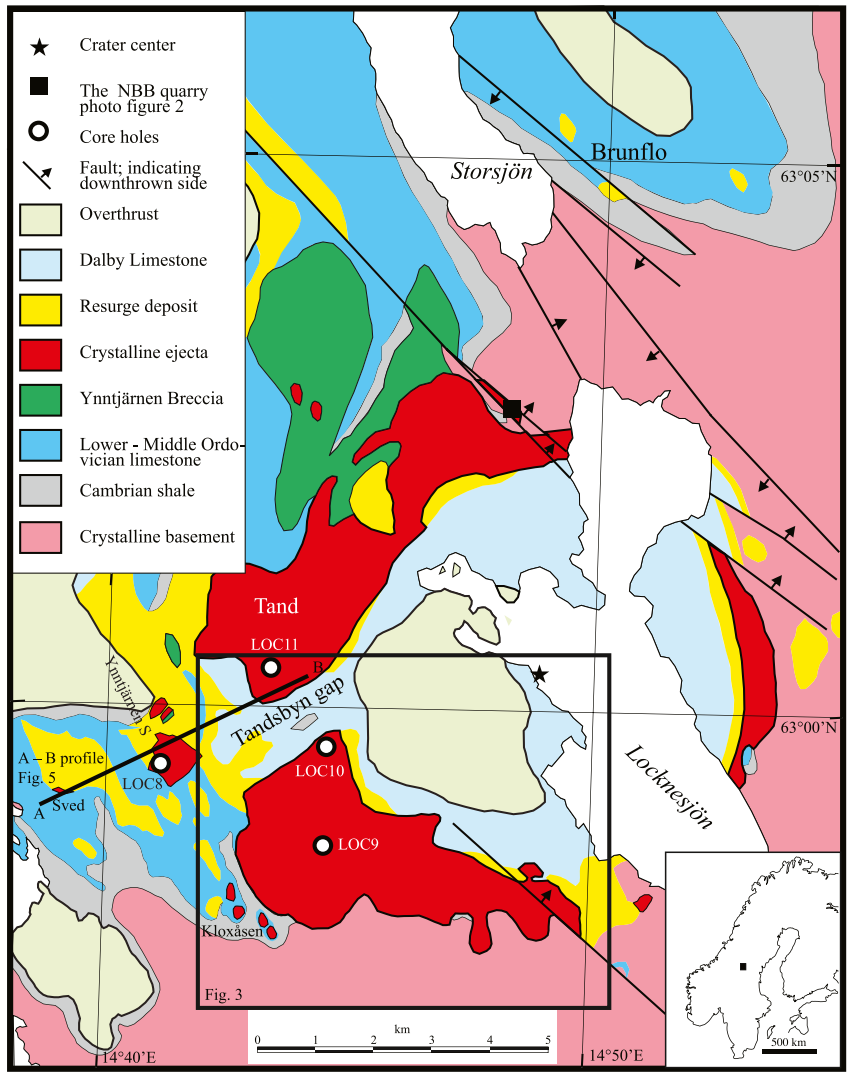


Figure 1. The geological map of the Lockne impact. Note the doublet Målingen crater is located 16 km to the southwest outside the map. The location of the Lockne area is given in the insert. The distribution of crystalline ejecta from the inner, nested, basement impact crater is given in red. The two largest proximal ejecta fields are the northern and southern, which are crescent-shaped. "The NBB quarry" indicates the location of the locality "Nordanbergsberget quarry." The geological profile A–B is presented in Figure 7.

in a depositional environment. The proximal ejecta around the 458 Ma marine-target Lockne impact structure (Figure 1) is well preserved and is probably one of the oldest intact proximal ejecta on Earth. The outline of the proximal ejecta has been shown to be pristine and influenced by the angle of impact with a trajectory from the East in today's cardinal directions (e.g., Lindström, Shuvalov, & Ivanov, 2005; Ormö et al., 2013). The reason for the good preservation of the ejecta layer is that the impact crater was overthrust by Caledonian nappes shortly after its formation. Later, erosion exposed the crater but only slightly affected its original morphology and preservation of impactites.

The target at Lockne consisted of a crystalline basement covered by approximately 80 m of sediments of varied degree of consolidation, as well as seawater of outer continental shelf depth due to the development of fore deep at the front of the Caledonian orogeny (i.e., ~500 m, Lindström, Ormö, et al., 2005; Lindström, Shuvalov, & Ivanov, 2005; Ormö et al., 2007). This layering of the target caused the impact crater to obtain what is known as a concentric impact crater (or nested impact crater) morphology (cf. Quaide & Oberbeck, 1968) with a 7.5 km wide, nested impact crater in the Precambrian crystalline target rock, surrounded by a ~14 km wide outer crater developed in the Lower Phanerozoic sedimentary sequence (e.g., Lindström, Ormö, et al., 2005; Ormö et al., 2013).

21699100, 2023, 7, Downloaded from https://agupubs.onlinelibrary.wiley.com/doi/10.1029/2023JE007777 by Csic Organización Central Om (Oficialia Mayor) (Urici), Wiley Online Library on [16/08/2023]. See the Terms and Conditions (https://onlinelibrary.wiley.com/terms-and-conditions) on Wiley Online Library for rules of use; OA articles are governed by the applicable Creative Commons License

21699100, 2023, 7, Downloaded from https://agupubs.onlinelibrary.wiley.com/doi/10.1029/2023JE007777 by Cnic Organización Central Om (Oficialia Mayor) (Unic), Wiley Online Library on [16/08/2023]. See the Terms and Conditions (https://onlinelibrary.wiley.com/terms-and-conditions) on Wiley Online Library for rules of use; OA articles are governed by the applicable Creative Commons License

The proximal ejecta is confined to the nested basement crater. There is no obvious ejecta layer preserved around the outer crater in the sedimentary sequence. Most likely, this ejecta mixed with the kilometer-high rim-wall of water (e.g., Lindström, Ormö, et al., 2005; Lindström et al., 2008), and was subsequently washed back toward the basement impact crater (Dalwigk & Ormö, 2001; Ormö et al., 2007). The proximal ejecta covering a continuous area north and south of the main impact crater is approximately 25 km^2 and is separated by an area almost completely void of continuous ejecta. This Tandsbyn gap, or "gully," was suggested by Lindström, Ormö, et al. (2005) to be the result of tangential rip apart during the ejecta displacement but has also been suggested to have been further shaped by the resurge erosion (Dalwigk & Ormö, 2001). The Tandsbyn gap is also indicated in the numerical simulation of basement crater ejecta distribution by Lindström, Shuvalov, and Ivanov (2005). However, the proximal ejecta on the down range side of the basement crater is more well developed than on the up-range side, which is expected for a 45° impact into the Lockne target configuration (cf. Lindström, Shuvalov, & Ivanov, 2005; Shuvalov et al., 2005). The proximal ejecta is almost entirely made up of material from the lover-most, crystalline part of the target as the excavation of the basement crater slightly succeeds the excavation of the outer crater in the sediments (e.g., Ormö et al., 2002; Shuvalov et al., 2005). The outward decreasing depth of the floor of the shallow outer crater leads to basement crater ejecta landing on outward progressively higher stratigraphic levels (Lindström, Ormö, et al., 2005; Lindström et al., 2008). The current estimate of the diameter of the outer crater (i.e., 14 km) is based on the extent of the semi-coherent basement crater ejecta masses and the numerical simulation results. A closer analysis of the nature and extent of this basement crater and its proximal ejecta is the subject of this study.

As our study focuses on the ejecta distribution around a medium-sized impact crater in a layered target, it is of interest to compare with some of the very few similar impact structures with preserved ejecta on Earth. One of the most studied and best-preserved impact craters with proximal ejecta is the 14.9 Ma Ries impact structure (e.g., Sturm et al., 2015). The thickest part of the proximal ejecta is deposited just beyond the crater rim and thins out exponentially with increasing distance (McGetchin et al., 1973; Melosh, 1989). In general, for impact craters, a proximal ejecta can be traced to about 1–2 crater radii beyond the crater rim (Melosh, 1989; Moore et al., 1974). In a sector including the elevated rim and to some extent beyond, the pre-existing stratigraphy of the target is preserved in detail but inverted and thinned. Jones (1978) denotes this as the "overturned flap." At the 74 Ma old and 37 km wide Manson impact structure in Iowa, USA (Katongo et al., 2004), this "overturned flap" comprises a major part of a zone of ejecta blocks in the continuous ejecta blanket (Witzke & Anderson, 1996). Sturm et al. (2015) describe large ejecta "megablocks" from the Ries impact structure as "coherent, lithologically homogenous blocks >25 m that were displaced and partly brecciated." In this study, we describe coherent crystalline ejecta bodies at the Lockne impact crater as equivalents to the "megablocks" described from Ries. These were introduced by Lindström, Ormö, et al. (2005) as "ejecta flaps" and can be partially still massive, fractured, or brecciated. The Manson impact structure formed in a mostly depositional environment and has a preserved proximal ejecta. However, the depositional environment also implies that the crater may be completely buried and inaccessible to ground studies. In contrast to Manson, which is accessible only through core drilling, the ejecta layer with its mega block zone at the Ries impact structure is both well-preserved and easily accessible (Sturm et al., 2015). The megablocks around the Ries impact structure originate from all stratigraphical levels, but most of the material (>80%) originates from the uppermost geological target unit of the Malmian age (Sturm et al., 2015, p. 156). Possibly, the production of mega blocks is dictated by the properties of the target rock, that is, some lithologies are more prone to flake up from the target than others. This could, for instance, be due to pre-existing fracture patterns or stratification of the target.

Beyond the continuous proximal ejecta, deposits are in general thin and patchy to a distance of about five crater radii beyond the crater rim. Further beyond lies the distal ejecta, which mainly appears as a thin layer of highly shocked material (Glass & Simonson, 2012).

Around the Lockne impact structure the mega-blocks of the overturned flap originate from the lowermost geological target unit, contrary to the situation around the Ries impact crater. This is most likely a consequence of a different mode of material emplacement at Lockne related to the shallow excavation flow that generated the outer impact crater surrounding the basement impact crater (cf. Shuvalov et al., 2005) and the circumstance that only material from the basement impact crater formed a preserved ejecta layer.

In many places in the Lockne basement impact crater, the proximal ejecta rest on the graphite bearing shale of mainly Cambrian age, which was inefficiently excavated during the outer crater formation (Sturkell et al., 2013).

21699100, 2023, 7, Downloaded from https://agupubs.onlinelibrary.wiley.com/doi/10.1029/2023JE007777 by Cnic Organización Central Om (Oficialia Mayor) (Unic), Wiley Online Library on [16/08/2023]. See the Terms and Conditions (https://onlinelibrary.wiley.com/terms-and-conditions) on Wiley Online Library for rules of use; OA articles are governed by the applicable Creative Commons License

The high electric conductivity of this shale gives a large contrast in resistivity, which is advantageous to this geoelectric study. Here, geological, and geophysical methods are used to describe the character (e.g., megablock sizes), distribution and stratigraphical position of the discordantly emplaced ejecta blanket around the basement crater of the Lockne concentric impact structure.

2. Geological Setting

The Lockne impact took place 458 Ma in 500 m deep ocean. The water depth has been estimated based on numerical simulation combined with geological and paleogeographical argumentation to be in the range of 500–700 m (Ormö et al., 2007; Shuvalov et al., 2005). However, detailed 3-D numerical simulation constrained by geological observation suggests a water depth in the lower end of the range, that is, approx. 500 m (Lindström, Shuvalov, & Ivanov, 2005). It is located on the Baltic Shield (Figure 1), on its (today) western edge that was pressed down as the collision with Greenland commenced, as the Caledonides were about to form (Heuwinkel & Lindström, 2007; Ormö et al., 2007). Due to the relatively rapid subsidence of the basement, the sedimentation at the time of the impact still belonged to the Central Baltoscandian Confacies Belt defined by Jaanusson (1976).

2.1. Impact-Generated Lithologies

At Lockne, there are two types of impact breccia: a breccia formed in the sediment layer;—the Ynntjärnen Breccia (Lindström, Ormö, et al., 2005), and a breccia formed in the crystalline basement—the Tandsbyn Breccia (Lindström and Sturkell, 1992). The Ynntjärnen Breccia is formed autochthonously to para-autochthonously and developed mainly by disruption of the consolidated limestone unit. Lindström et al. (2008) proposed the genesis by a combination of basement crater ejecta bombardment combined with high-speed water movements during the excavation flow (i.e., "water blow ejecta") as well as pounding and seismic shaking from the collapse of the kilometer-high water cavity rim. Large bodies of Ynntjärnen Breccia can be seen to have been disintegrated by the resurge and incorporated into the Lockne Breccia (coarse clastic) and Loftarstone (arenitic) resurge deposits (Dalwigk & Ormö, 2001). The 40 m of dark mud or clay between the limestone and the crystalline basement could not be brecciated. However, it was liquefied and slumped into the impact crater before the water resurge during the crater modification stage, forming a slump breccia—the Tramsta Breccia (Sturkell et al., 2013). Nevertheless, during the shallow excavation of the outer crater the clay could behave as a cohesive material hard to displace, like chewing gum on table, and remain smeared over the outer crater floor to become covered by crystalline basement crater ejecta.

2.2. Near Field Ejecta

The ejecta clasts generated by the impact appear in all sizes from sub-mm to several tens of meters across. At Lockne, the largest preserved ejecta clasts originate from the crystalline target rock dominated by granites. The crystalline target within the crater damage zone shows a span from being completely brecciated to only slightly fractured. The impact breccia in the crystalline rock, the Tandsbyn Breccia, forms instantly at impact and has even been observed to have been ejected as coherent large (tens of meters) bodies of breccia (e.g., Melero-Asensio et al., 2014). Similar bodies of Tandsbyn Breccia, albeit much smaller, are also seen as part of the resurge breccia, thus creating a "breccia in breccia" (Lindström et al., 1996). No similarly large ejecta blocks of limestone have been observed. The upper, limestone part of the target at the direct impact site was likely both vaporized and ejected as smaller ejecta fragments to a higher degree than the deeper basement rocks. If mega blocks of bedded limestone were formed, they are embedded in the Ynntjärnen Breccia (the impact breccia in the sediment succession) and, thus, hard to distinguish.

The Tandsbyn gap separates the northern and the southern ejecta fields (Figure 1). The southern field with proximal ejecta is possible to map with a fairly good accuracy, as the soil cover is thin. The part with crystalline rocks (fractured and brecciated) often protrudes over the lower lying swamps and bogs. When exposed, the lower contact of the crystalline breccia commonly rests upon shale. It is the low permeability of the shale that underlies the swamps that causes their formation over the otherwise brecciated substrate. This facilitates the mapping of the extent of shale over the areas with ejecta, especially in the southern ejecta sector. In the northern ejecta sector, the soil cover is of much greater thickness, which is expressed in today's cultivated areas as well as forest where most of the swamps have been drained.

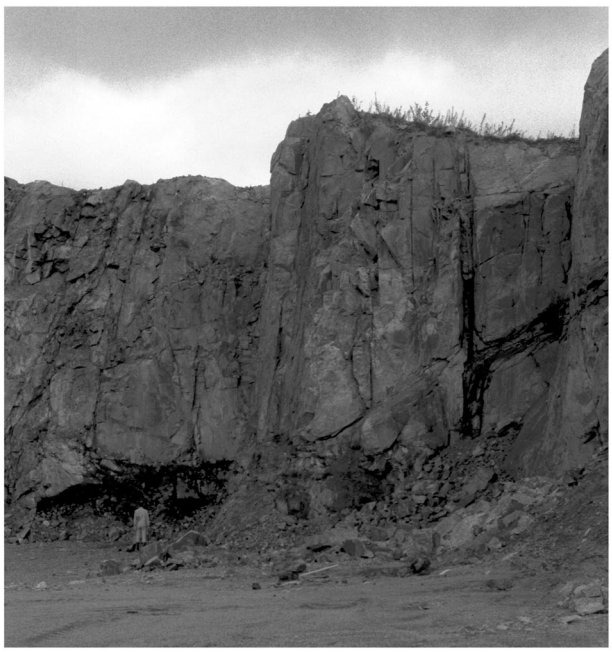


Figure 2. Rock wall of the Nordanbergsberget quarry in pre-Cambrian granite, in which the granite rests on Cambrian shale. At the time of the impact, the Cambrian sediments were un-lithified, and the clay was squeezed into cracks in the granite. The peneplain is located near the base of the quarry at 375 m above sea level. A 1.9 m tall man standing in front of the black Cambrian shale in the lower right part of the photograph.

On the eastern edge of the northern crescent-shaped ejecta field, a quarry is located (Figure 1) where a pre-Cambrian 1.8–1.9 Ga granite is being extracted (Högdahl, 2000). Simon (1987a) reported the occurrence of Cambrian shale under 15–20 m thick granite in the then newly opened quarry. This location is close to the nested crater rim, and it appears that the granite mega block is at least 800 meter long and 200 meter wide. This mega block represents an "overturned flap" as the block still has the lower most meter of the Cambrian succession inverted resting upon a normal succession of lowermost meter of the Cambrian succession. In general, just outside the impact disturbed area, the Cambrian succession is approximately 30 m thick, as can be seen at, for instance, Brunflo (Figure 1). The Cambrian dark mud that today forms the shale could at the time of impact easily be squeezed into cracks (Figure 2). In the northern ejecta area at a farm called Tand (Figure 1), a drilling for water struck Cambrian shale at 50 m depth under granite (Sturkell & Lindström, 2004). This constrains the level of the sub-Cambrian peneplain in the area. However, in the nearby drilling LOC11, the shale was not encountered at the respective level, which indicates local variations in the depth of brecciation.

Only minor occurrences of ejected material are found on the eastern, up range, side of the crater (Figure 1) (see review by Ormö et al., 2013).

2.3. Post Impact Influence on the Crater

Directly after the sediment transport of the resurge had ceased, the silt and clay fraction could settle out of the water column before the deposition returned to the normal background sedimentation. The post impact sedimentation in Jämtland continued mostly uninterrupted until the lower Silurian (Jaanusson, 1982).

The Caledonian orogeny started to influence the Lockne area in the early Ordovician when the western (today) edge of the Baltic Shield was pressed down. This is demonstrated with the regional facies variation from east to west (Jaanusson, 1982).

The overthrusting by the Caledonian orogeny shortened the area covered by discontinuous proximal ejecta to the west of the Lockne impact structure (Lindström et al., 1996; Sturkell et al., 2000). The structure became covered by about 5 km of overthrusts, of which today an outlier in the central parts of the crystalline impact crater bare witness (Figure 1). The two large fields of proximal ejecta seem to have been spared of any major nappe disturbance and instead they seem to have behaved as an obstacle for the lowest nappes (Lindström, Ormö, et al., 2005). The peak of the orogeny took place in Mid-Late Silurian and the Early Devonian.

The post impact faulting occurred during and after the Caledonian orogeny. The dominating fault motion is vertical, only with minor strike slip components. The east of Lockne Lake (Figure 1) has been down faulted almost 100 m (Sturkell & Lindström, 2004). This has helped to preserve the impact structure on the eastern shore of the lake (Figure 1). A graben structure strike NNW to SSE in the continuation of the outline of Lake Storsjön in Figure 1. The observation of resurge sediments resting on an un-brecciated crystalline basement on the eastern margin of the crater. East of the impact structure at the margin of the graben, the highest hill in the crystalline rocks rises about 100 m above the eastern margin of the impact structure.

3. Methods

3.1. Core Drilling

In the Lockne impact structure, 11 core drillings have been performed since the 1990s. Four of them (LOC08-11, Table 1 and Figure S2–S4 in Supporting Information S1) start in crystalline ejecta and penetrate below the calculated level of the peneplain (cf. Sturkell & Lindström, 2004).

The names given to the drill cores and core holes at Lockne can vary between different publications as well as depending on available size in map presentations. For instance, a core called "Lockne-8" may also appear as "LOC08" (used in this study). This study makes use of data from these short core drillings (Figure 1) as

21699100, 2023, 7, Downloaded from https://agupubs.onlinelibrary.wiley.com/doi/10.1029/2023JE007777 by Cnic Organización Central Om (Oficialia Mayor) (Unic), Wiley Online Library on [16/08/2023]. See the Terms and Conditions (https://onlinelibrary.wiley.com/terms-and-conditions) on Wiley Online Library for rules of use; OA articles are governed by the applicable Creative Commons License

Table 1
Core Holes in the Lockne Area That Starts in Crystalline Ejecta and are Expected to Penetrate the Peneplain

Drill hole	E-W (m)	N-S (m)	Height (m.a.s.l.)	Length	Termination depth	Peneplain level	Alum shale interval	Position along resistivity profile
LOC08	1,443,471	6,987,107	420.3	52.2	366.5	340.6	36–49	2:21/3:1
LOC09	1,446,489	6,986,070	400.0	31.0	369.0	386.6	23–28	3:17
LOC10	1,445,910	6,987,570	382.5	46.0	336.5	367.1	19–35	2:19
LOC11	1,445,425	6,988,374	401.7	62.2	339.5	354.4	None	4:17

Note. The Alum shale appears as matrix in these drill cores. The location of the peneplain at each drill site is calculated by the equation of the plane $6.353682x - 4.207748\ y - 512.3452z + 20{,}403{,}144.0 = 0$, where x, y, and z are given in meters, from Sturkell and Lindström (2004). The height refers to the elevation of the surfaces at the site. The result of the LOC09 drilling is given in Melero-Asensio et al. (2014). The drillings were performed by the company Drillcon Core AB stationed in Nora, Sweden.

constraints for the analysis of the geophysical data. In two instances, we use drill cores (i.e., LOC08 and LOC09) that were retrieved already in 2004 as the subject of those drillings also was to investigate the thickness and properties of the crystalline ejecta deposits. Only LOC09, however, has so far been described in publications (i.e., Lindgren et al., 2007; Melero-Asensio et al., 2014). The other two cores mentioned here, LOC10 and LOC11, were retrieved for this study with the use of the same type of equipment as for LOC08 and LOC09. The core log descriptions presented here are in line with the aim of the study, that is, to determine the thickness and main lithological composition of the ejecta and do, thus, not provide all additional information that would be possible to obtain from the material (e.g., Lindgren et al., 2007; Melero-Asensio et al., 2014). The LOC08 core hole was located at the center of a large solitary ejecta body that occupies the outer reach of the Tandsbyn gap. The LOC09 core hole was located at the center of the south-western coherent ejecta field at a position coinciding with the cross-section of the crater drawn by Lindström, Ormö, et al. (2005). The LOC10 core hole was in the north-western ejecta field at a position just outside the flank of the Tandsbyn gap, and the LOC11 core hole was located in a similar position just to the south of the Tandsbyn gap so that they would facilitate the reconstruction of a transverse geological cross-section of this gap in the proximal ejecta.

3.2. Mapping

The proximal ejecta including mega-blocks (i.e., the flaps) forming the two crescent-shaped main areas (Figure 1) was mapped out in detail. Mapping was carried out by Maurits Lindström, his students, and by the two first authors Erik Sturkell and Jens Ormö. The two areas are, however, different in several respects: degree of exposure, till cover, number of settlements, and the number (area) of bogs between the outcropping ejecta blocks. The northern area has much fewer outcrops than the southern, which is due to the thicker till and soil cover. Likewise, the area covered by bogs is much smaller compared to the southern area. The southern area has a better exposure of outcrops, in particular of fractured crystalline and Tandsbyn Breccia (Figure 3). The soil cover is thin (<0.5 m or absent). No cultivated land occurs in the southern ejecta field (Figure 4). Habitation is only located just beyond the proximal ejecta (e.g., Klocksåsen, Figure 1).

The geological mapping was combined with LIDAR topography data with an altitude resolution of 2 cm. This data was made by the Swedish geodetic services (Lantmäteriet) and obtained from the server at the Swedish University of Agricultural Sciences.

The geological mapping of the proximal ejecta fields hints that marsh and bog areas frequently coincide with areas of impermeable shale, that is, remnants of lower sedimentary target below the ejecta layer. Thus, they also occur as "windows" through the ejecta with an altitude often coinciding with the level of the peneplain. The bogs are easily detectable as flat surfaces in the Lidar data. Appling the outcrop's location together with the bogs reveals that the small hills between the bogs consist of crystalline rocks (fractured or brecciated). At the base of the hills, shale crop out at several places. A frequent morphological feature is a cavity at the base of the crystalline hill due to later partial erosion of the shale. This feature is so-far only observed in the southern area.

21699100, 2023, 7, Downloaded from https://agupubs.onlinelibrary.wiley.com/doi/10.1029/2023JE007777 by Csic Organizacion Central Om (Oficialia Mayor) (Ulrc), Wiley Online Library on [16/08/2023]. See the Terms and Conditions (https://onlinelibrary.wiley.com/terms-and-conditions) on Wiley Online Library for rules of use; OA articles are governed by the applicable Creative Commons License

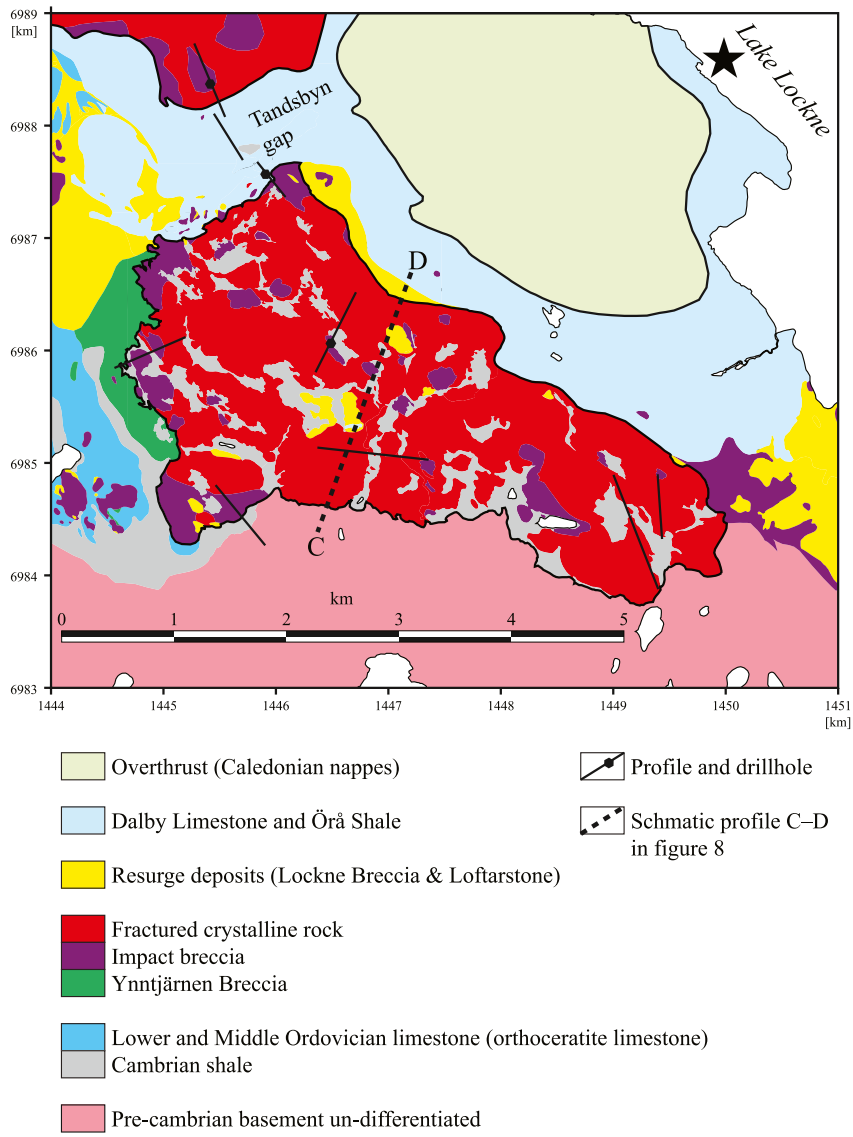


Figure 3. A detailed geological map of the southern proximal ejecta and the Tandsbyn gap. The gap forms a down range opening through the basement impact crater rim. In the southern proximal ejecta field fractured and brecciated crystalline rock rest upon the floor of the outer impact crater, which is a surface stripped by a shallow excavation flow to outwards progressively higher stratigraphic levels. In addition to direct outcrop observations, the distribution of shale is suggested from the topography as well as strong link to swampy areas. The numbers of the profiles and the drill sites are given in Figure 4. The coordinates are in the grid system RT 90, the official Swedish name for a transverse Mercator projection.

3.3. Resistivity Profiles

The resistivity data were collected with an ABEM Terrameter LS-CVES instrument along 11 profiles of variable length from 400 to 1600 m. The distance between the electrodes was 5 m and a roll along strategy was adapted for longer profiles than 400 m. To correct for the effect of topography, each profile was leveled using a Sokkisha C3E. Profiles close to a benchmark altitude point from the Geodetic Survey of Sweden get correct absolute values, but for most of the profiles, a perfect tie to a benchmark point was not possible. In these cases, the Lidar-height model was used. However, the relative height differences along all profiles are correct with centimeter precision. The resistivity measurements were performed during the summers 2013 to 2016 by Erik Sturkell, Jens Ormö, Eric Hegardt, Gabrielle Stockmann, Erik Meland, Åsa Frisk, and Pierre Etienne Martin.

21699100, 2023, 7, Downloaded from https://agupubs.onlinelibrary.wiley.com/doi/10.1029/2023JE007777 by Csic Organización Central Om (Oficialia Mayor) (Urici), Wiley Online Library on [16/08/2023]. See the Terms and Conditions (https://onlinelibrary.wiley.com/terms-and-conditions) on Wiley Online Library for rules of use; OA articles are governed by the applicable Creative Commons License

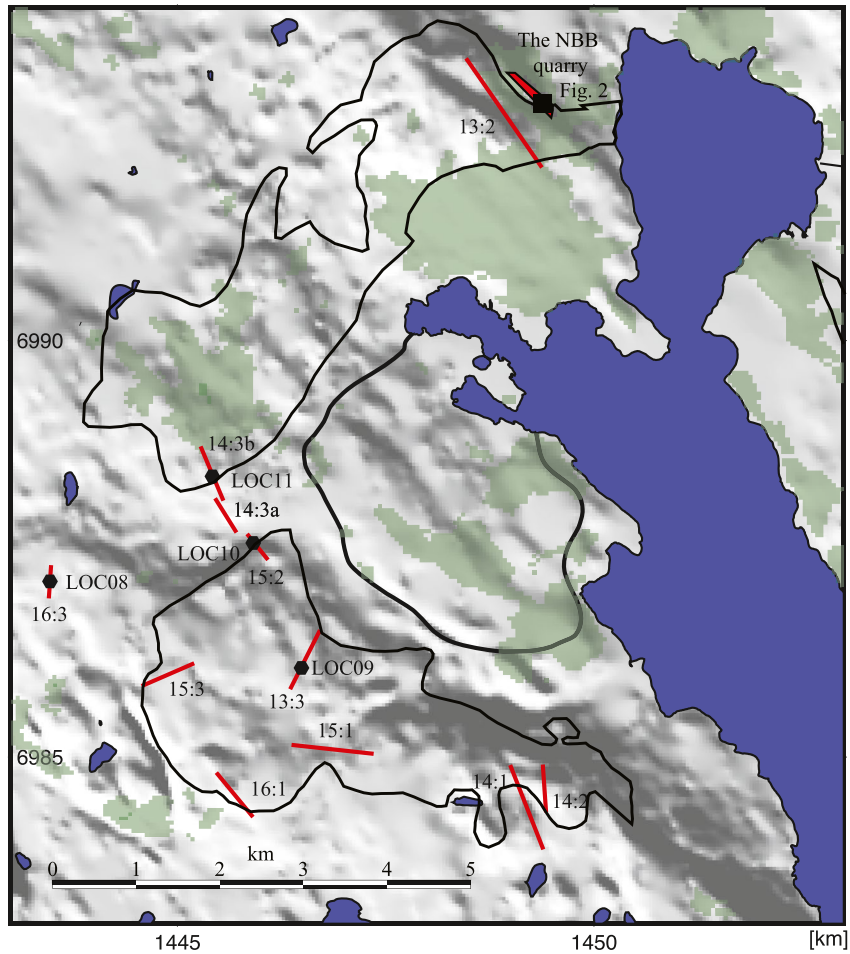


Figure 4. The background is a sun-shaded map of topography, the green area is open farmland (data from the Swedish geodetic services (Lantmäteriet)). Map showing the locations of the resistivity profiles and the drill sites. Some of the resistivity profiles intersect one or more drill sites. Profile 13:2 in the north is parallel to the ridge of the Nordanbergsberget quarry. The green-shaded areas are open farmland, which indicates the thickness of the soil layer. This results in poorer exposure of outcrops. The black line shows the outline of the two (i.e., the northern and southern) crescent-shaped, continuous ejecta fields. The black lines represent the major geological boundaries for the ejecta and the nappe in the center of the structure, from Figure 1. The coordinates are in the grid system RT 90, the official Swedish name for a transverse Mercator projection.

Data processing was made with the software Res2Dinv version 3.5 from Geotomo Software and the result is presented in a pseudo section. Data for the Res2Dinv processing, the number of iterations run and the absolute error are given in Table S2 in Supporting Information S1.

After the processed resistivity data were corrected for the topography, the results are presented in pseudo profiles along with interpretations shown in Figures 5a–5c. The processed resistivity data were sorted into ranges and connected to respective lithologies. To present a calculation and inversion of electrical measurements as a function of position (x, y, z) and electrode separation, the apparent resistivity is presented in a so-called pseudosection.

3.4. VLF Resistivity and Fracture Frequency

In 2002 resistivity measurements and fracture frequency measurements were made by Ann Bäckström and Jens Ormö over the crystalline ejecta areas to determine the degree of fracturing and brecciation. The resistivity measurements were made with a Very Low Frequency (VLF) EM 16R instrument from Geonic equipped with an additional 10 m-long antenna that is laid out over the ground. The instrument measures the ratio between the electric and magnetic fields and gives the phase angle and the apparent resistivity (ρ_a). In addition to a

21699100, 2023, 7, Downloaded from https://agupubs.onlinelibrary.wiley.com/doi/10.1029/2023JE007777 by Csic Organización Central Om (Oficialia Mayor) (Uricv), Wiley Online Library on [16/08/2023]. See the Terms and Conditions (https://onlinelibrary.wiley.com/terms-and-conditions) on Wiley Online Library for rules of use; OA articles are governed by the applicable Creative Commons License

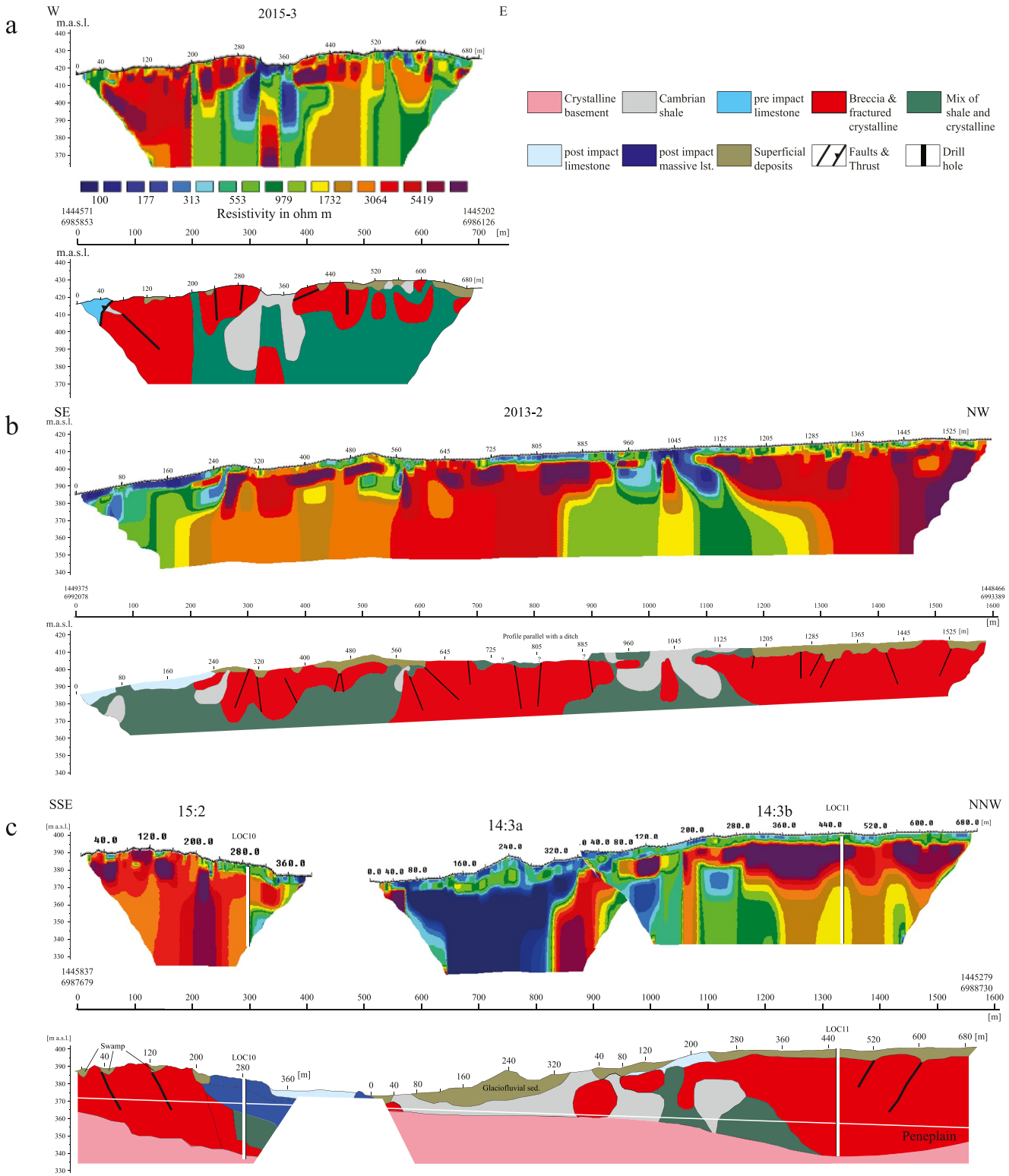


Figure 5.

21699100, 2023, 7, Downloaded from https://agupubs.onlinelibrary.wiley.com/doi/10.1029/2023JE007777 by Csic Organización Central Om (Oficialia Mayor) (Ulrci), Wiley Online Library on [16/08/2023]. See the Terms and Conditions (https://onlinelibrary.wiley.com/terms-and-conditions) on Wiley Online Library for rules of use; OA articles are governed by the applicable Creative Commons License

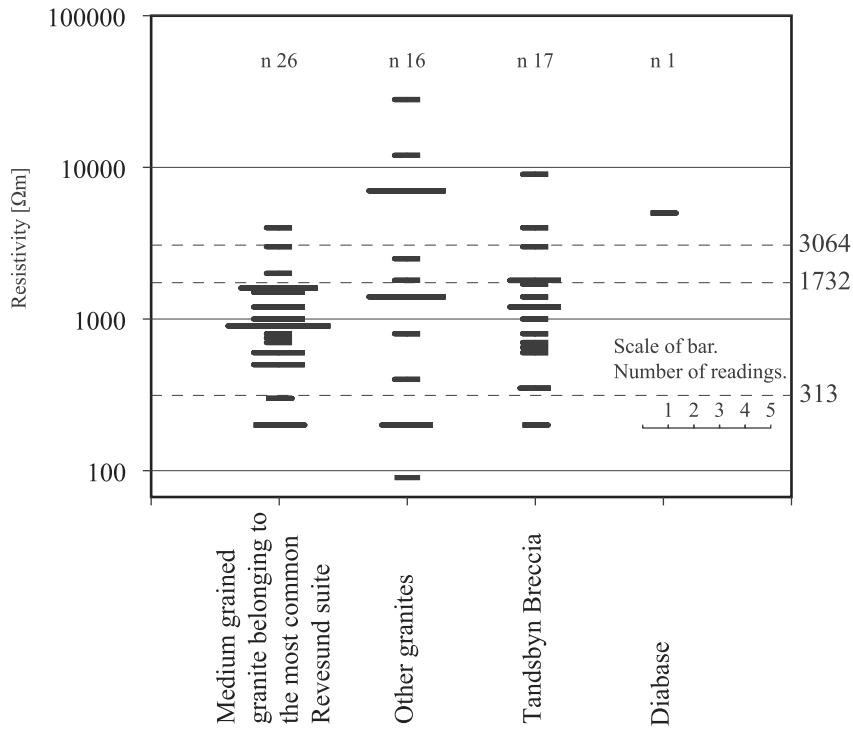


Figure 6. A tree diagram showing the distribution of resistivity values in the crystalline ejecta split into four groups depending on the area around the crater. The dashed horizontal lines show resistivity values given in the pseudo profiles. The data originate from Bäckström (2005). The resistivity measurements were made with a Very Low Frequency EM 16R instrument from Geonic equipped with an additional 10 m-long antenna that is laid out over the ground.

top layer (here crystalline ejecta), a deeper positioned layer can also be detected if it occurs within the VLF skin-depth. The fracture frequencies were measured over a set 1 m^2 surface. Some of the results were published in Bäckström (2005), but other previously unpublished data. In connection with the field work that led to the Bäckström (2005) article additional resistivity measurements were performed in locations outside two profiles described by Bäckström (2005). These data cover a larger area of the ejecta and are considered of interest to this study. A large portion of the measurements were performed around the quarry (Nordanbergsberget). The resistivity measurements were made on medium grained granite, undifferentiated granite, the direct impact breccia in the crystalline basement (Tandsbyn Breccia), and on one dolerite out-crop (Figure 6).

4. Results

4.1. Core Drilling and Mapping

The proximal ejecta field was drilled at three sites LOC09-11. The LOC09 and 10 penetrate through a section of a mixed zone of Cambrian shale and fragmented crystalline. In both drillings, the encountered level of the expected (calculated, see Table 1) peneplain was within 10 m. Also, for LOC09 and LOC10, the shale was found under crystalline breccia, confirming that the breccias are allochthonous ejecta masses. The schematic drill logs are provided in Supporting Information S1.

Figure 5. The scale for resistivity pseudo sections, length scale, and the legend for the interpreted section are identical for all profiles (see location on Figure 4). Top panel depicts the resistivity data, and the lower panel shows the interpreted geological profiles based on the resistivity measurements, outcrop observations and core holes. (a) A west to east resistivity pseudo profile and the interpretation for the 2015-3 section (see location on Figure 4) that runs across a shallow valley. At the western side of the valley (at 320 m distance), next to the swamp, Cambrian shale is cropping out. The granitic ejecta flap is interpreted to consist of several blocks. (b) A 1600 m long resistivity profile (2013-2), which stretches parallel to the elongated crystalline ridge at the quarry (Figures 1 and 4). The peneplain is in the base of the quarry (Figure 2) at 360 m level, which is in the lowermost part of the south–eastern end of the profile. (c) Resistivity profile across the Tandsbyn gap valley is composed of three individual profiles that have been combined (Figure 4). A railroad and a road in the lowermost part of the valley prohibit a continuation of the profile. Two core-holes are located along the profile. To the south-southeast, the crystalline mega blocks rest on the pre-Cambrian target but to uncertain depths.

21699100, 2023, 7, Downloaded from https://agupubs.onlinelibrary.wiley.com/doi/10.1029/2023JE007777 by Cslc Organización Central Om (Oficialia Mayor) (Uric), Wiley Online Library on [16/08/2023]. See the Terms and Conditions (https://onlinelibrary.wiley.com/terms-and-conditions) on Wiley Online Library for rules of use; OA articles are governed by the applicable Creative Commons License

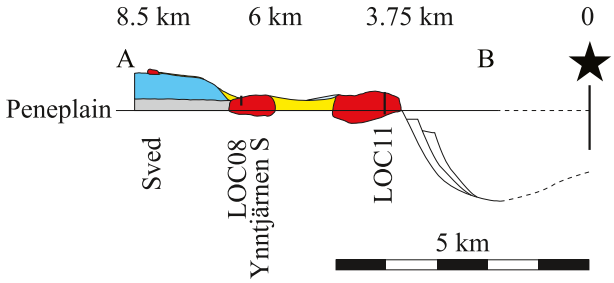


Figure 7. Profile from the center of the impact crater in the down range direction at approximately 250° bearing (for locations see Figure 1).

The entire 61.5-m long LOC11 drill core reveals brecciated medium grained granite from top to bottom. The drill hole terminates at 339 m.a.s.l. approximately 15 m below the expected level of the peneplain without having encountered it.

In the LOC10 drilling, a 30 cm thick sandstone dike is found at the 339 m.a.s.l. (43 m depth in the drill core) equaling a level 27 m below the peneplain. Also, a <10 cm thick sandstone dyke is found at the 347 m level (35 m in drill core). This is a new occurrence of clastic injections complementing the seven that have been previously described by Sturkell and Ormö (1997).

Outside the proximal ejecta field, there are sporadic occurrences of huge blocks of crystalline rock (fractured to completely brecciated). Lindström, Ormö, et al. (2005, p. 377) list 12 large clasts, which are distributed between Ynntjärnen in the North and Kloxåsen in the South (Figure 1). Ejecta blocks are mainly located at the outer edge of the proximal ejecta field in the down range area (Lindström, Ormö, et al., 2005). The circumstance that the proximal ejecta field rests upon outwards progressively higher stratigraphic levels leads to that the outer edge of the proximal ejecta (≈5.6 km from crater center) rests upon lower Ordovician beds. Beyond the edge, and to a distance of 6.5–6.8 km from the center at Kloxåsen (Figure 1), crystalline ejecta rest on lower and middle Ordovician strata (Sjöqvist et al., 2017). Three large crystalline ejecta megablocks are in the direct downrange direction; of these the largest is the "Ynntjärnen S" (Figure 7) that has an estimated volume of 2×10^5 m^3 (Lindström, Shuvalov, & Ivanov, 2005) and lies at 6.4 km from the center. This is penetrated by the 53.8 m long LOC8 drill hole, ending approximately 26 m above the calculated peneplain level (Table 1). The core shows mainly crystalline breccia all the way to the bottom, however, interrupted by approximately 3 m of limestone breccia in the upper third part. There is no obvious peneplain encountered in the core, although alum shale occurs dispersed in the matrix from about 36 m depth and downwards. Likewise, the cores LOC10 and 11 display brecciated crystalline continuously down to the end of the core holes, here tens of meters below the expected level of the peneplain. In LOC10, there are sporadic occurrences of alum shale at a depth coinciding with the calculated level of the peneplain, but in LOC11, there is no indication that the core reaches into the autochthonous basement. Thus, it seems that the crystalline ejecta at this location has either penetrated all the way down into the basement or has an indistinguishable contact to an underlying strongly brecciated basement (Figure 7).

The crystalline ejecta masses at Sved (Figure 7) are located 8.6 km from the center and with a volume of 5×10^4 m^3 (Lindström, Ormö, et al., 2005). This ejecta megablock rests only approximately 5–6 m below the target level in the limestone succession, that is, on beds belonging to the upper Middle Ordovician conodont zone *Pyg. serra* (Simon, 1987b, p. 68).

Numerical simulation supported (Lindström, Shuvalov, & Ivanov, 2005; Shuvalov et al., 2005) by the circumstance that the sedimentary target succession of the outer crater was eroded by the early stage shallow excavation flow, indicating that the full extent of the outer crater was essentially freed of water at the moment of deposition of the basement crater crystalline ejecta. The expelled water formed a steep, up to 2 km high, wall at the outer limit of the excavated cavity (e.g., Lindström, Shuvalov, & Ivanov, 2005; Shuvalov et al., 2005). The numerical simulation by Lindström, Shuvalov, and Ivanov (2005) likewise shows that the basement crater ejecta could not readily penetrate beyond the wall of water. Indeed, if ejecta would strike the water column, it is unlikely that it would maintain enough energy to penetrate through both water and the mainly consolidated sedimentary target succession and into the basement. Thus, the secondary cratering around the Lockne crater must have been formed by ballistic ejecta striking the dry floor of the outer crater.

By using the distribution of crystalline ejecta that have cratered the sedimentary target sequence, the outline of the water crater can be drawn. It supports the previous assumption (i.e., Ormö et al., 2013) that the water crater must be wider in the down range direction (toward the west).

21699100, 2023, 7, Downloaded from https://agupubs.onlinelibrary.wiley.com/doi/10.1029/2023JE007777 by Cátc Organización Central Om (Oficialia Mayor) (Utrc), Wiley Online Library on [16/08/2023]. See the Terms and Conditions (https://onlinelibrary.wiley.com/terms-and-conditions) on Wiley Online Library for rules of use; OA articles are governed by the applicable Creative Commons License

4.2. Fracture Frequency From VLF and Literature Data

In a study by Bäckström (2005), it is observed that the non-brecciated crystalline rock has a resistivity >10,000 Ωm. It is also seen that the resistivity of brecciated crystalline rock ranges between 300 and >10,000 Ωm (Figure 6). This is consistent with surface measurements of mapped ejecta masses. Bäckström (2005) also measured the fracture frequency in the crystalline (granite) rock along two radial profiles emanating from the crater center and crossing over the ejecta zone and beyond it. The rocks along the northern profile located 1 km west of the quarry (Nordanbergsberget) has a fracture frequency of about 1,000/m^2. This profile does not reach beyond the proximal ejecta field. The second, southern profile starts in the crystalline proximal ejecta field with a fracture frequency of 1,000/m^2. The first 500 m of the profile is within the proximal ejecta field. The following 500 m shows a decline of the fracture frequency ramping off to about 100/m^2 and is here continuing outside the proximal ejecta where the fracture frequency of the crystalline basement rock drops to about 10/m^2.

4.3. Resistivity Profiles

A selected collection of representative pseudo section with interpretation is given in Figures 5a–5e; additional data are available in Supporting Information S1.

It is of special importance to this study that the Cambrian mud was carbon rich in combination with being affected by heat during the Caledonian orogeny transforming it to a shale. The maximum temperature inflicted did not exceeded 300°C (Sturkell et al., 1998) but was enough to transform the carbon into graphite, a highly conductive material. This indicates that the shale today has a very low resistivity, often less than 100 Ωm.

The resistivity profiles across the proximal ejecta show the distribution of crystalline mega blocks and the Cambrian shale occurring below the ejecta and squeezed in-between major coherent blocks. The measured resistivities range from 1 to more than 10,000 Ωm and are subdivided into four groups; The lowest resistivity <313 Ωm group includes water and shale. The 313–1,732 Ωm group represents a mixed lithology of shale and granite (breccia), mainly ejected material from the crystalline basement that bombarded the exposed Cambrian clay and become intermixed with it. An example of this mixing can be observed in the LOC10 drill-core (Figure 1), where granitic clasts rest in a clay (today shale) matrix. The third (1,732–3,064 Ωm) and fourth (>3,064 Ωm) groups represent granite with a decreasing number of fractures. The resistivity of the Tandsbyn Breccia can span over the three first groups as it may include the full spectrum from clasts separated by open fractures to types that are massive (Figure 6). Törnberg and Sturkell (2005) showed how the density of the Tandsbyn Breccia varies with the amount of matrix.

In the resistivity profiles, areas with values >1,732 Ωm consist of more or less fractured crystalline (granite). This lithology reaches up close to the surface, indicating a thin layer of superficial deposits. Along the profiles, in particular at their lower parts, swamps are frequent and are characterized by very low resistivities. The intersected swamps are indexed in the interpreted profiles (e.g., the middle of profile 2015-3 Figure 5a). At some parts of the profiles a thin layer (<5 m) with resistivity ranging from 1 to 3,064 Ωm occurs on top of a body with higher resistivity (>3,064 Ωm) This is probably a mixture with small swamps and glacial till. At some parts of the profiles (Figure 5 and profile 16-1 in Supporting Information S1) shale was observed at the surface that could be connected with the lower resistivities. This suggests that at other profiles with no obvious swamp, a body of low resistivity instead probably is related to shale. Likewise, deeper located low-resistivity bodies are most probably shale. Occasionally, as in profile 2013-2, an elongated body of low resistivity also probably relates to shale (i.e., mud at the time of impact) that has been squeezed up in voids between the mega blocks (Figures 5a–5c).

Along the profile, crystalline rock is exposed at surface, which corresponds to the high resistivity parts. To the extreme west, pre-impact limestone appears, and the contact is interpreted to be at a Caledonian thrust. This pre-impact limestone has been strongly affected by the impact (i.e., Ynntjärnen Breccia). In this section, shale was observed to crop out under the crystalline rock at the western side of the valley seen at the center of the profile. This valley also hosts several swamps as the shale decreases the water permeability into the underlying fractured rock. The resistivity around 500 most likely represents a mixture of shale and crystalline rocks. Several mega blocks can be singled out embedded in the shale—crystalline mixture. No clear basement peneplain can be distinguished.

21699100, 2023, 7, Downloaded from https://agupubs.onlinelibrary.wiley.com/doi/10.1029/2023JE007777 by Cstc Organización Central Om (Oficialia Mayor) (Unic), Wiley Online Library on [16/08/2023]. See the Terms and Conditions (https://onlinelibrary.wiley.com/terms-and-conditions) on Wiley Online Library for rules of use; OA articles are governed by the applicable Creative Commons License

On the valley slope, a bedded post-impact limestone crops out, while at the bottom of the valley, different facies of the same limestone are exposed. In the central part of the profile, Cambrian shale forms a low resistivity body. This shale occurrence is confirmed by surface observations by Thorslund (1940). The low-resistivity shale conceals all rock units below it. The third profile (14:3b in Figure 5c) exhibits from left to right blocks of high resistivity resting on top of low-resistivity shale and a mix of shale and crystalline material. Toward the north-northwest, a huge mega block has penetrated down in the calculated position of the pre-Cambrian peneplain. This interpretation is based on the out-come of the drilling LOC11.

4.4. Estimates of Ejecta Volumes

In the 26 km wide Ries impact structure, reconstruction suggests that the mega blocks originate from a 14–15 km wide transient crater and have an estimated volume of 47 km^3 (Sturm et al., 2015). At the 7.5 km wide basement crater of the Lockne impact structure, the continuous proximal ejecta covers an area of 25 km^2 and some additional mega blocks with a combined area of 1 km^2. Using an average thickness of 30 m gives a volume of the ejecta masses of about 0.8 km^3, which is a fifth of the volume of the Ries mega block ejecta. No limestone mega block ejecta has been identified so far. The circumstance that the Lockne impact took place in an approximate 500 m deep ocean had the effect that a large proportion of the ejected material consisted of water. This severely reduced the volume of the ejected crystalline material. We estimate that much of the finer ejecta (~<1,000 m^3) have been re-deposited by the resurge. Simon (1987b, pp. 90–91) performed an extensive (>40 thin sections) component analysis of the fine grained resurge deposits (<-3φ) that showed that 25–30 vol% of the material originates from the crystalline target. Sturkell and Lindström (1996) estimated that 13 km^3 of resurge deposits would have been deposited within a radius of 50 km from the impact center. Thus, the fine-grained parts of the resurge (i.e., the Loftarstone) deposits would consist of 3–4 km^3 of material from the crystalline target. Loftarstone constitutes the majority of the resurge deposits over the crystalline proximal ejecta but is still showing a thin (<some meters) and patchy distribution. That this represents, more or less, the fresh post-impact distribution and thickness of the resurge deposits over the basement ejecta flaps is confirmed by how some of the deposits are overlaid by post impact secular sediments (Figure 3). But more important for this study is that the resurge deposits overlaying the ejecta masses show that the thickness of the ejecta field can be considered pristine.

Notwithstanding the differences in proportions between ejecta- and displacement-zones between the 7.5-km wide nested basement crater of Lockne, formed in the lower part of the target succession, and that of an equal-sized crater in a homogeneous crystalline target, we may still attempt to make a rough estimate of how much of the total volume of excavated basement that today is visible as preserved near-proximal ejecta. First, the amount of excavated material from a crater can be calculated based on the relation given in Melosh (1989, p. 78). Where the excavated depth $H_{exc} \approx 1/3H_t \approx 1/10D_t$, where H_t the depth of the transient crater and D_t the diameter of the transient crater at target surface. Likewise, the ratio of the observed crystalline proximal ejecta volume of the total calculated excavated volume can be estimated. From the numerical simulations of the crater development of the Lockne impact presented by Lindström, Shuvalov, and Ivanov (2005, Figure 3, 10 s-time frame), we obtain a D_t of 6 km. The excavated depth is then calculated to be (H_{exc}) 1/10 × 6 = 0.6 km. For simplicity, we consider that the excavated part of the crater is in the shape of a spherical cap. The volume of a spherical cap is $V_{cap} = 1/6\ \pi\ h(3a\text{^}2 + h\text{^}2)$ with the height (h) and the radii (a) corresponding to that height (if calculating the volume of a half sphere $h = a$). The excavated depth is 0.6 km and the radii are $a = 6/2 = 3$ km. Applying this simplified shape ($1/6\pi$ 0.6 (3 × 3^2 + 0.6^2)) gives an estimated excavated volume of 5.16 km^3. Of this volume, approximately 75 vol% is deposited as near proximal ejecta field beyond the rim (Melosh, 1989, p. 90). This gives a calculated amount of 3.9 km^3 of near proximal ejecta field around the nested basement impact crater of Lockne. This can then be compared with the estimated volume of the here studied crystalline ejecta field, which is ≈1 km^3. Thus, the preserved proximal ejecta today is (1/3.9) × 100, representing 26 vol% of the estimated excavated material. However, possibly, the lower position of the nested basement crater relative to the target succession (i.e., 500 m of water and 80 m of sediments) may cause the excavated zone of the crater to be relatively small compared to the displacement zone. Therefore, the 26 vol% may be considered to represent a lower limit.

21699100, 2023, 7, Downloaded from https://agupubs.onlinelibrary.wiley.com/doi/10.1029/2023JE007777 by Csic Organización Central Om (Oficialia Mayor) (Utrc), Wiley Online Library on [16/08/2023]. See the Terms and Conditions (https://onlinelibrary.wiley.com/terms-and-conditions) on Wiley Online Library for rules of use; OA articles are governed by the applicable Creative Commons License

The remaining 74 vol% of crystalline ejecta would occur as clasts within the resurge deposits of which much are today preserved only within the nested basement crater (e.g., Ormö et al., 2007; Sturkell et al., 2013) and as more distal deposits over the surrounding seafloor of which today only the locality Hallen is known at a distance of 45 km from Lockne (Sturkell et al., 2000). At this location, abundant up to 15 cm large granite clasts occur in an up to 40 cm thick bed of resurge deposits in the otherwise nearly complete sedimentary sequence.

5. Discussion

The concentric shape of the Lockne impact structure is a consequence of the layered target. Numerical simulations by Valery Shuvalov (i.e., Lindström, Shuvalov, & Ivanov, 2005; Ormö et al., 2002; Shuvalov et al., 2005) indicate that the outer impact crater surrounding the 7.5 km inner crater would be at the most approximately 14 km wide, possibly with a downrange offset of a couple of km (Ormö et al., 2013). This is, however, not enough to explain the great extent of basement crater ejecta in the down-range direction. Ormö, Sturkell, Alwmark, and Melosh (2014) speculate if it may be the projectile properties that have caused the outer crater to be much more extensive, especially downrange, than what the simulations have indicated. They argue that while the numerical simulations have been calculated with a monolithic massive projectile, the projectile would instead have been poorly consolidated and prone to separate into a broad pancake-shaped cluster. This argument is based on the circumstance that the 600 m diameter "Lockne" asteroid had a 150m diameter satellite. This satellite created the Målingen impact crater some 16 km SW of Lockne (Ormö, Sturkell, Nõlvak, et al., 2014). Thus, the combined Lockne—Målingen structure is the result of a doublet impact from a binary asteroid (Ormö, Sturkell, Alwmark, & Melosh, 2014). As most binaries in this size-range are so-called "rubble pile" asteroids, this was most likely the case for the Lockne-Målingen impact (Ormö, Sturkell, Alwmark, & Melosh, 2014). A 600 m rubble pile projectile would experience a deformation into a wide cluster due to aerodynamic friction. Highly simplified, one could compare the impact of such a possible clustered projectile with the wide, but shallow crater caused by a shotgun blast. It is possible that the effect is accentuated by the obliquity of impact (Ormö, Sturkell, Alwmark, & Melosh, 2014; Schultz & Gault, 1985).

The excavation of the basement crater and the deposition of the basement crater ejecta until the outer reach of the outer crater (approx. 7 km from the crater center) span a time sequence of about 100 s (Lindström, Shuvalov, & Ivanov, 2005). The ejecta layer consists of large coherent masses of crystalline breccia (Tandsbyn Breccia), which in many cases seem to have been solidified before transport, creating huge (tens of meters) blocks of "breccia-in-breccia." Although much of the Cambrian and lower–most Ordovician clays were stripped from the floor of the expanding outer crater, some were trapped under the overturned ejecta flaps near the crater rim and could slump into the fresh crater (Sturkell et al., 2013).

As the area of "proximal" ejecta is larger than the source area, Lindström, Shuvalov, and Ivanov (2005) suggest that a geometric tangential spreading occurs that makes gaps between larger ejecta bodies. These, sometimes hundreds of meters wide, rip-apart structures may in turn have channeled the resurge flow leading to additional expansion by erosion (cf. Dalwigk & Ormö, 2001; Lindström, Shuvalov, & Ivanov, 2005). We anticipate that the same tangential spread occurs at all scales, and that it has generated extensional fractures (Figure 8) in which clay has been squeezed up (Figure 2). The tangential stresses during the ejecta emplacement show that the process was not a perfect radial ballistic emplacement of a particulate material. The relatively wide flaps of crystalline rock with a low degree of fracturing observed in our resistivity measurements and at the cross-section of the quarry at Nordanbergsberget, as well as the large mega-blocks of breccia seemingly solidified prior to deposition, support that the ejecta was constituted by rock masses of some strength that were ripped apart.

At the outer rim of the crater, the proximal ejecta was overridden by the resurge and probably all the fragments small enough to be picked up by the currents were swept into the crater. While the resurge deposits were very thin over the coherent basement ejecta masses, most of the resurge deposition occurred within the nested basement crater (e.g., Ormö et al., 2007 and references therein). The resurge deposits filled the cracks between the ejecta masses (Figure 3), which can reach thicknesses of more than 30 m. As only a rather small amount of the more high-energy, coarse grained resurge deposits (i.e., Lockne breccia) are preserved in-between the ejected mega-blocks, the main deposition of resurge material over the basement ejecta masses, flaps and crater rim must have occurred at the final stage of the resurge. Probably, the crater rim areas were the place with the highest veloc-

21699100, 2023, 7, Downloaded from https://agupubs.onlinelibrary.wiley.com/doi/10.1029/2023JE007777 by Csic Organización Central Om (Oficialia Mayor) (Urici), Wiley Online Library on [16/08/2023]. See the Terms and Conditions (https://onlinelibrary.wiley.com/terms-and-conditions) on Wiley Online Library for rules of use; OA articles are governed by the applicable Creative Commons License

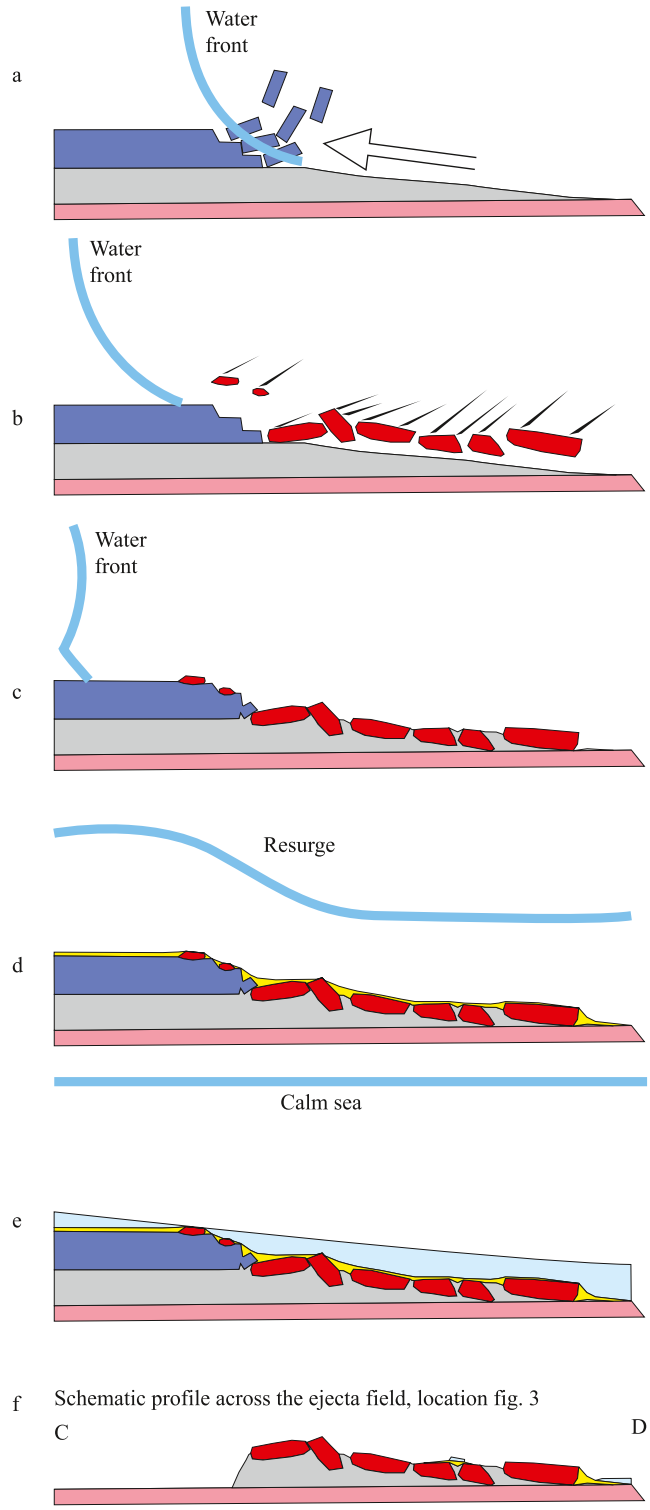


Figure 8. The suggested sequence for the formation of the ejecta field along a profile across the southern ejecta field (see Figure 3). For lithological legend, see Figure 3. (a) Expansion of the outer crater due to shallow excavation flow. (b) Inner crater basement ejecta striking the floor of the outer crater. (c) The moment of initiation of resurge flow from the collapsing water cavity. (d) Deposition of resurge material (yellow) over the ejecta layer. (e) Post impact secular sedimentation of marine Dalby Limestone. Blue line shows the position of the water cavity. For a more extensive explanation, see the last paragraph of the Section 5.

21699100, 2023, 7, Downloaded from https://agupubs.onlinelibrary.wiley.com/doi/10.1029/2023JE007777 by Csic Organización Central Om (Oficialia Mayor) (Urici), Wiley Online Library on [16/08/2023]. See the Terms and Conditions (https://onlinelibrary.wiley.com/terms-and-conditions) on Wiley Online Library for rules of use; OA articles are governed by the applicable Creative Commons License

ity of the resurge, allowing deposition mainly inside the inner crater itself during most of the resurge process. As the resurge velocities decreased, the Loftarstone draped the area, which still had a lot of topography. Finally, the post impact Dalby limestone and younger sediments covered all of the area.

In the Lockne mega block zone, more than 90% of the material originates from the lowermost part of the target. This is totally opposite to the situation at the Ries impact structure, where close to 80% of the mega blocks originate from the uppermost stratigraphic unit in the target, the Malmian (Sturm et al., 2015, p. 156). In the Lockne impact structure, only two parts of the target are strong enough to potentially produce mega blocks: the bedded limestone and the crystalline basement. In the proximal ejecta around Lockne, in particular the south-western part, the ejecta originates from the crystalline basement as the limestone had already been stripped from the target by the shallow excavation flow producing the outer crater before cratering commenced in the basement part of the target (e.g., Lindström, Ormö, et al., 2005). The outer crater does not have a rim wall with accumulated ejecta, so it is not possible to say if the bedded limestone produced any megablocks. The ejecta from the outer crater instead blended with the huge amount of expelled seawater and, as it seems, were disintegrated into smaller (<meter size) blocks during the resurge.

At the eastern side of the crater, resurge rocks rest directly on the Precambrian peneplain, and the zone of crystalline ejecta is much narrower and thinner than on the western side of the crater. Here, it measures only a few hundred meters in width and a few meters in thickness. Only one megablock has been found on the eastern side of the Lockne structure. The reason for this may be either; (a) that no mega-block was ejected in that direction, or (b) that the mega-blocks have been eroded. However, similar to the western ejecta, the proximal ejecta thickness is constrained by theoccurrences of Loftarstone resurge deposits. Instead, numerical simulation by Shuvalov et al. (2005) indicates that the ejection of basement crater ejecta on the up-range side of the crater is much subdued and at a steeper angle than on the downrange side. The outer uprange crater rim wall of water would have, likewise, been steeper and standing much nearer to the basement crater rim. Thus, the first alternative is favored. In the northeastern sector, a few crystalline ejecta (mega-blocks) are observed resting on a progressively higher stratigraphical level with increasing distance (Sturkell, 1998a). Toward the northeast, at the municipally of Brunflo, the pre-impact Palaeozoic strata are preserved. In the sequence that is not severely disturbed by the Caledonian nappes, a sloping surface with progressively deeper erosion into the Ordovician and Cambrian layers toward the crater is described by Sturkell (1998b), who interpreted it as a morphology generated by resurge erosion. However, the circumstance that crystalline ejecta occurs between the cut surface through the Paleozoic sequence and overlying resurge deposits demonstrates that the surface is the floor of the outer crater formed by the early shallow excavation flow.

The ejecta clast farthest to the west at Sved (Figure 7) is resting on the top of the pre-impact succession, which fits well with the general pattern the farther out the higher in the stratigraphy. Obviously, the crystalline ejecta in this westward direction, that is, the LOC11, must have penetrated through the whole Paleozoic sequence as there is no trace of Cambrian Shale at those sites. The drilling LOC08 at "Ynntjärnen S" furthest to the west terminates 26 m above the peneplain level. The lower 40 m of this drilling penetrates a mixture of shale and crystalline material. This is interpreted as "squeezed" material between the ejecta clasts (e.g., Figure 2).

The impact angle influences the ejecta distribution more than the crater morphology (Melosh, 1989, p. 101). At Lockne, the downrange proximal ejecta field reaches 2.5 km beyond the crater rim; this is ≈2/3 the crater radius. Continuous ejecta normally extends about 1–2 crater radii from the crater rim (Melosh, 1989, p. 90), which, thus, indicates some additional mechanism in play during the cratering at Lockne. Possibly, in marine impacts, the water wall may pose an obstacle for the nested crater ejecta. When this ejecta interacts with the water wall (Figure 8), they lose velocity (i.e., kinetic energy) and have a shorter trajectory. Most likely, ejecta bodies also disintegrate upon impact with the water wall. Therefore, the position of the water wall will inhibit the ejecta distribution and the ability for secondary catering of the surrounding surfaces.

Figure 8 describes the conceptual process of the ejecta flap development as reconstructed from the geophysical profiles and geological mapping presented here. The process has been subdivided into a few steps although it is continuous:

Figure 8a: Some of the outgoing shallow excavation flow follows the boundary beds between the clay and the lithified limestone, rolling up brittle limestone like a carpet (cf. Sturkell & Ormö, 1997). The more ductile mud and clay of the lower sedimentary target are, however, not as easily removed and came to cover the floor of the

21699100, 2023, 7, Downloaded from https://agupubs.onlinelibrary.wiley.com/doi/10.1029/2023JE007777 by Csic Organización Central Om (Oficialia Mayor) (Utrc), Wiley Online Library on [16/08/2023]. See the Terms and Conditions (https://onlinelibrary.wiley.com/terms-and-conditions) on Wiley Online Library for rules of use; OA articles are governed by the applicable Creative Commons License

21699100, 2023, 7, Downloaded from https://agupubs.onlinelibrary.wiley.com/doi/10.1029/2023JE007777 by Cnic Organización Central Om (Oficialia Mayor) (Unic), Wiley Online Library on [16/08/2023]. See the Terms and Conditions (https://onlinelibrary.wiley.com/terms-and-conditions) on Wiley Online Library for rules of use; OA articles are governed by the applicable Creative Commons License

inner parts of the outer crater. Figure 8b: The crystalline ejecta hit the floor of the newly formed outer crater (Ormö, Sturkell, Alwmark, & Melosh, 2014). A so-called "water blow breccia" (i.e., Ynntjärnen Breccia) forms by the high-energy water-jet and crystalline ejecta striking the lithified limestone part of the target sequence (cf. Lindström et al., 2008). Closer to the crater, remnant mud and clay are impacted by the basement crater ejecta and blend in as matrix around the clasts in a transition zone between ejecta and basement (cf. LOC9 drill core, Melero-Asensio et al., 2014. For location, see Figure 1). The Cambrian clay squeezes up between major coherent ejecta masses ("mega blocks"), and/or slumps down into the basement crater (cf. Sturkell et al., 2013). An example of mud injections is seen at location Nordanbergsberget in Figure 2. Figure 8c: The inner part of the basement impact crater where the proximal ejecta rests on the soft clay and mud. In the area further out, the ejecta rests on brecciated limestone (Ynntjärnen Breccia). The induced outward motion and the weight of the ejecta masses might cause a tilt of the limestone beds adjacent to the ejecta masses. Large ejecta masses strike with high kinetic energy and may penetrate deep into the sedimentary target strata (e.g., the Klocksåsen ejecta masses, see Lindström et al., 1983; Sjöqvist et al., 2017; Sturkell, 1998a) and even down into the basement, as observed at LOC11 (Figures 1 and 5c). Figure 8d: The resurge flow leaves a relatively thin cover of reworked ejecta and rip-up material (yellow) over the proximal ejecta. Note the more discontinues extent of the southern proximal ejecta in the southern sector (Figure 3.) The resurge deposits are intercalated between the ejecta and the post impact Dalby Limestone (the yellow field in Figures 3 and 8e). On the other hand, the resurge deposits are of great thickness (several tens of meters) in the interior of the crater (e.g., Lindström, Ormö, et al., 2005; Lindström et al., 1996; Ormö et al., 2007). Figure 8e: The post impact secular sediments (i.e., Dalby limestone) are deposed in several different facies (Frisk & Ormö, 2007) depending on the topographic location on the elevated rim as well as variations in the substrate, but this is not differentiated in this figure.

6. Conclusions

The proximal ejecta around the Lockne impact structure is well preserved and has a pristine distribution dominantly in the shape of two crescents with a bias toward the NW and SW separated by an area where ejecta is absent, possibly a so-called "forbidden zone" indicating an oblique impact from the east. The southern proximal ejecta field reaches the farthest, that is, approximately 7 km from the impact crater center.

The crystalline ejecta covers an area of 26 km^2, for which all but one km^2 is within the two crescent-shaped proximal ejecta fields. Proximal parts of the ejecta rest upon basement or Cambrian shale as the Ordovician limestone was stripped by the shallow excavation flow. Ejecta lies on stratigraphically higher positions outward from the nested crater.

The impact breccias (Tandsbyn Breccia) and the fractured crystalline rock have similar high resistivity values. The resistivity of the crystalline mega blocks is normally exceeding 1,000 Ωm and are commonly >3,000 Ωm in many cases. On the other hand, the Cambrian shale has a resistivity of about 100 Ωm or less, clearly distinguishing it from the crystalline material. If the low resistivity layer occurs in the topmost position, it will conceal all other lithologies below. However, in most cases, the high resistivity lithologies occur on top, which allows the thickness of the ejecta to be distinguished.

Data Availability Statement

Additional maps, processed resistivity profiles, and tables with data are available in a repository. The raw data of the resistivity measurements are available in the repository too (Sturkell et al., 2023).

Acknowledgments
Åsa Frisk and Pierre Etienne Martin, who helped with the field measurements are greatly acknowledged. We thank Ann Bäckström for the resistivity data she made available for this study. Harald Olsson, who passed away in February 2021, lived on the edge of the impact structure in Ångsta at the farmed named Nordanberg. He took great interest in promoting the Lockne impact structure and helped researchers coming to the area. Furthermore, he took the initiative to build up the Lockne impact museum in Ångsta. The work by Jens Ormö and Erik Sturkell was supported by Grant PID2021-125883NB-C22 by the Spanish Ministry of Science and Innovation/State Agency of Research MCIN/AEI/https://doi.org/10.13039/501100011033 and by "ERDF A way of making Europe," as well as the Spanish Research Council (CSIC) support for international cooperation I-LINK project ILINK22061. The authors are grateful for the valuable comments by Christian Koeberl and an anonymous reviewer.

References

Bäckström, A. (2005). A study of impact fracturing and electric resistivity related to Lockne impact structure, Sweden, the Mora meeting proceedings. In C. Koeberl & H. Henkel (Eds.), *Impact tectonics* (pp. 389–404). Springer-Verlag.

Dalwigk, I. V., & Ormö, J. (2001). Formation of resurge gullies at impacts at sea: The Lockne crater, Sweden. *Meteoritics & Planetary Sciences*, *36*(3), 359–370. https://doi.org/10.1111/j.1945-5100.2001.tb01879.x

Frisk, Å. M., & Ormö, J. (2007). Facies distribution of post- impact sediments in the Ordovician Lockne and Tvären impact craters: Indications for unique impact generated environments. *Meteoritics & Planetary Sciences*, *42*(11), 1971–1984. https://doi.org/10.1111/j.1945-5100.2007.tb00554.x

Glass, B. P., & Simonson, B. M. (2012). *Distal impact ejecta layers: A record of large impacts in sedimentary deposits* (p. 716) Springer Science & Business Media. https://doi.org/10.1007/978-3-540-88262-6

Heuwinkel, J., & Lindström, M. (2007). Sedimentary and tectonic environment of the Ordovician Föllinge Greywacke, Storsjön area, Swedish Caledonides. *GFF*, *129*(1), 31–42. https://doi.org/10.1080/11035890701291031

Högdahl, K. (2000). 1.86–1.85 Ga intrusive ages of K-feldspar megacryst-bearing granites in the type area of Revsund granites in Jämtland County, central Sweden. *GFF*, *122*(4), 359–366. https://doi.org/10.1080/11035890001224359

Jaanusson, V. (1976). Faunal dynamics in the middle Ordovician (Viruan) of Balto-Scandia. In M. G. Bassett (Ed.), *The ordovician system: Proceedings of a palaeontological association symposium* (pp. 301–326). University of Wales Press.

Jaanusson, V. (1982). Introduction to the Ordovician of Sweden. In D. H. Bruton & S. H. Williams (Eds.), *IV. International symposium on the Ordovician system. Field excursion guide, palaeontological contributions from the University of oslo* (Vol. 279, pp. 1–9).

Jones, G. H. S. (1978). Coherently overturned flaps surround craters. *Nature*, *273*(5659), 211–213. https://doi.org/10.1038/273211b0

Katongo, C., Koeberl, C., Witzke, B. J., Hammond, R. H., & Anderson, R. R. (2004). Geochemistry and shock petrography of the Crow Creek Member, South Dakota, USA: Ejecta from the 74-Ma Manson impact structure. *Meteoritics & Planetary Sciences*, *39*(1), 31–51. https://doi.org/10.1111/j.1945-5100.2004.tb00048.x

Lindgren, P., Parnell, J., Norman, C., Mark, D. F., Baron, M., Ormö, J., et al. (2007). Formation of Uranium/thorium-rich bitumen nodules in the Lockne impact crater, Sweden: A mechanism for carbon concentration at impact sites. *Meteoritics & Planetary Sciences*, *42*(11), 1961–1989. https://doi.org/10.1111/j.1945-5100.2007.tb00553.x

Lindström, M., Ormö, J., & Sturkell, E. (2008). Water-blow and resurge breccias at the Lockne marine-target impact structure. In I. K. Evans, J. W. Horton, D. T. King, & J. R. Morrow (Eds.), *GSA special paper* (Vol. 437, pp. 43–54). https://doi.org/10.1130/2008.2437(03)

Lindström, M., Ormö, J., Sturkell, E., & Dalwigk, I. V. (2005). The Lockne crater: Revision and reassessment of structure and impact stratigraphy. In C. Koeberl & H. Henkel (Eds.), *Impact tectonics* (pp. 357–388). Springer-Verlag.

Lindström, M., Shuvalov, V., & Ivanov, B. (2005). Lockne crater as a result of marine-target oblique impact. *Planetary and Space Science*, *53*(8), 803–815. https://doi.org/10.1016/j.pss.2005.02.005

Lindström, M., Simon, S., Paul, B., & Kessler, K. (1983). The Ordovician and its mass movements in the Lockne Area near the Caledonian margin, central Sweden. *Geologica et Palaeontologica*, *17*, 17–27.

Lindström, M., & Sturkell, E. F. F. (1992). Geology of the early Palaeozoic Lockne impact, central Sweden. *Tectonophysics*, *216*(1–2), 169–185. https://doi.org/10.1016/0040-1951(92)90164-2

Lindström, M., Sturkell, E. F. F., Törnberg, R., & Ormö, J. (1996). The marine impact crater at Lockne, central Sweden. *GFF*, *118*(4), 193–206. https://doi.org/10.1080/11035899609546255

McGetchin, T. R., Settle, M., & Head, J. W. (1973). Radial thickness variation in impact crater ejecta: Implications for lunar basin deposits. *Earth and Planetary Science Letters*, *20*(2), 226–236. https://doi.org/10.1016/0012-821x(73)90162-3

Melero-Asensio, I., Martin-Hernandez, F., & Ormö, J. (2014). A rock magnetic profile through the ejecta flap of the Lockne impact crater (central Sweden) and implications for the impact excavation process. *Journal of Applied Geophysics*, *112*, 91–105. https://doi.org/10.1016/j.jappgeo.2014.11.009

Melosh, J. (1989). *Impact cratering—A geologic process*. Oxford University Press.

Moore, H. J., Hodges, C. A., & Scott, D. H. (1974). Multiringed basins—Illustrated by Orientale and associated features. In *Abstract at the 5th lunar science conference* (pp. 71–100).

Ormö, J., Rossi, A. P., & Housen, K. R. (2013). A new method to determine the direction of impact: Asymmetry of concentric impact craters as observed in the field (Lockne), on Mars, in experiments, and simulations. *Meteoritics & Planetary Sciences*, *48*(3), 403–419. https://doi.org/10.1111/maps.12065

Ormö, J., Shuvalov, V., & Lindström, M. (2002). Numerical modeling for target water depth estimation of marine-target impact craters. *Journal of Geophysical Research*, *107*(E12), 31–39. https://doi.org/10.1029/2002je001865

Ormö, J., Sturkell, E., Alwmark, C., & Melosh, J. (2014). First known terrestrial impact of a binary asteroid from a main Belt Breakup event. *Scientific Reports*, *4*(1), 6724. https://doi.org/10.1038/srep06724

Ormö, J., Sturkell, E., & Lindström, M. (2007). Sedimentological analysis of resurge deposits at the Lockne and Tvären craters: Clues to flow dynamics. *Meteoritics & Planetary Sciences*, *42*(11), 1929–1944. https://doi.org/10.1111/j.1945-5100.2007.tb00551.x

Ormö, J., Sturkell, E., Nõlvak, J., Melero-Asensio, I., Frisk, Å., & Wikström, T. (2014). The geology of the Målingen structure: A probable doublet to the Lockne marine-target impact crater, central Sweden. *Meteoritics & Planetary Sciences*, *49*(3), 313–327. https://doi.org/10.1111/maps.12251

Osinski, G. R., Tornabene, L. L., & Grieve, R. A. F. (2011). Impact ejecta emplacement on terrestrial planets. *Earth and Planetary Science Letters*, *310*(3–4), 167–181. https://doi.org/10.1016/j.epsl.2011.08.012

Quaide, W. L., & Oberbeck, V. R. (1968). Thickness determinations of the lunar surface layer from lunar impact craters. *Journal of Geophysical Research*, *73*(16), 5247–5270. https://doi.org/10.1029/jb073i016p05247

Schultz, P. H., & Gault, D. E. (1985). Clustered impacts: Experiments and implications. *Journal of Geophysical Research*, *90*(B5), 3701–3732. https://doi.org/10.1029/jb090ib05p03701

Shuvalov, V., Ormö, J., & Lindström, M. (2005). Hydrocode simulation of the Lockne marine target impact event. In C. Koeberl & H. Henkel (Eds.), *Impact tectonics* (pp. 405–422). Springer-Verlag.

Simon, S. (1987a). Caledonian deformation of basement in the Lockne area, Jämtland, central Sweden. *Geologiska Foreningens I Stockholm Forhandlingar*, *109*(4), 269–273. https://doi.org/10.1080/11035898709453088

Simon, S. (1987b). Stratigraphie, Petrographie und Entstehungsbedingungen von Grobklastika in der autochthonen, ordovizischen Schichtenfolge Jämtlands (Schweden). *Sveriges geologiska undersökning C*, *815*, 1–156.

Sjöqvist, A. S. L., Lindgren, P., Sturkell, E. F. F., Hogmalm, K. J., Broman, C., Ivarsson, M., & Lee, M. R. (2017). Shock metamorphism and hydrothermal alteration of mafic impact ejecta from the Lockne impact structure, Sweden. *GFF*, *139*(2), 119–128. https://doi.org/10.1080/11035897.2016.1227361

Sturkell, E., & Lindström, M. (2004). The target peneplain of the Lockne impact. *Meteoritics & Planetary Sciences*, *39*(10), 1721–1731. https://doi.org/10.1111/j.1945-5100.2004.tb00068.x

Sturkell, E., Ormö, J., Hegardt, E. A., Stockmann, G., Meland, E., & Wikström, T. (2023). Data repository. https://doi.org/10.5878/mqt8-x135

Sturkell, E., Ormö, J., & Lepinette, A. (2013). Early modification stage (preresurge) sediment mobilization in the Lockne concentric, marine-target crater, Sweden. *Meteoritics & Planetary Sciences*, *48*(3), 321–338. https://doi.org/10.1111/maps.12058

Sturkell, E., Ormö, J., Nõlvak, J., & Wallin, Å. (2000). Distant ejecta from the Lockne marine-target impact crater, Sweden. *Meteoritics & Planetary Sciences*, *35*(5), 929–936. https://doi.org/10.1111/j.1945-5100.2000.tb01482.x

Sturkell, E. F. F. (1998a). The marine Lockne impact structure, Jämtland, Sweden: A review. *Geologische Rundschau*, *87*(3), 253–267. https://doi.org/10.1007/s005310050208

21699100, 2023, 7, Downloaded from https://agupubs.onlinelibrary.wiley.com/doi/10.1029/2023JE007777 by Csic Organización Central Om (Oficialia Mayor) (Unlc), Wiley Online Library on [16/08/2023]. See the Terms and Conditions (https://onlinelibrary.wiley.com/terms-and-conditions) on Wiley Online Library for rules of use; OA articles are governed by the applicable Creative Commons License

Sturkell, E. F. F. (1998b). Resurge morphology of the marine Lockne impact crater, Jämtland, central Sweden. *Geological Magazine*, *135*(1), 121–127. https://doi.org/10.1017/s0016756897007875

Sturkell, E. F. F., Broman, C., Forsberg, P., & Torssander, T. (1998). Impact-related hydrothermal activity in the Lockne impact structure, Jämtland, Sweden. *European Journal of Mineralogy*, *10*(3), 589–606. https://doi.org/10.1127/ejm/10/3/0589

Sturkell, E. F. F., & Lindström, M. (1996). Mass balance of the Lockne impact structure, central Sweden. In *Abstract at current problems, ideas, and results in geology stockholm, GFF 118, Jubilee issue* (pp. A102–A103).

Sturkell, E. F. F., & Ormö, J. (1997). Impact-related clastic injections in the marine Ordovician Lockne impact structure, central Sweden. *Sedimentology*, *44*(5), 793–804. https://doi.org/10.1046/j.1365-3091.1997.d01-54.x

Sturm, S., Kenkmann, T., Willmes, M., Pöosges, G., & Hiesinger, H. (2015). The distribution of 488 megablocks in the Ries crater, Germany: Remote sensing, field investigation, and 489 statistical analyses. *Meteoritics & Planetary Sciences*, *50*(1), 141–171. https://doi.org/10.1111/maps.12408

Thorslund, P. (1940). On the Chasmops series of Jemtland and Södermanland (Tväre n). *Sveriges Geologiska Undersökning C*, *494*, 1–191.

Törnberg, R., & Sturkell, E. F. F. (2005). Petrophysics of marine Lockne and Tvären impact structures. *Meteoritics & Planetary Sciences*, *40*(4), 639–651. https://doi.org/10.1111/j.1945-5100.2005.tb00968.x

Witzke, R. J., & Anderson, R. R. (1996). Sedimentary-clast breccias of the Manson impact structure. In C. Koeberl & R. R. Anderson (Eds.), *The Manson impact structure, Iowa: Anatomy of an impact crater, geological society of America special paper, Boulder, Colorado* (Vol. 302, pp. 115–144).

21699100, 2023, 7, Downloaded from https://agupubs.onlinelibrary.wiley.com/doi/10.1029/2023JE007777 by Cnic Organización Central Om (Oficialia Mayor) (Unic), Wiley Online Library on [16/08/2023]. See the Terms and Conditions (https://onlinelibrary.wiley.com/terms-and-conditions) on Wiley Online Library for rules of use; OA articles are governed by the applicable Creative Commons License